Temperature (in)dependence of the Casimir-Polder potential of a particle near a metallic sphere

Simen Å. Ellingsen
Department of Energy and Process Engineering, Norwegian University of Science and Technology, N-7491 Trondheim, Norway

Stefan Yoshi Buhmann and Stefan Scheel
Quantum Optics and Laser Science, Blackett Laboratory, Imperial College London, Prince Consort Road, London SW7 2BW, United Kingdom

(Dated: July 13, 2011)

It has recently been shown that the Casimir-Polder potential of a particle in an energy eigenstate near a conducting body can be virtually temperature independent, provided the separation between particle and body is small enough so that retardation effects are negligible. In the present paper we study the leading residual temperature dependence due to retardation and imperfect conductivity for an atom near a metal sphere. For this prototype of a curved geometry, we obtain a closed-form expression for the temperature-dependent potential which is found numerically to be an excellent approximation.

PACS numbers: 31.30.jh, 12.20.–m, 34.35.+a, 42.50.Nn

I. INTRODUCTION

Recent times have witnessed a blossoming of experimental set-ups holding great promise, in which the detailed interaction of particles with nearby surfaces is important. Some such systems are not necessarily in thermal equilibrium, such as Bose-Einstein condensates in magnetic traps close to surfaces [1], beams of cold polar molecules [2] and Rydberg atoms [3]. In the conventional literature on London-van der Waals forces [4] and its more general version, the Casimir-Polder (CP) forces [5], it has, with some notable exceptions, been common to assume thermal equilibrium (for reviews, c.f. Refs. [6, 7]), so a description of these important experimental situations demanded a new theory. For a full theoretical background of different non-equilibrium Casimir-Polder scenarios the reader may refer to Refs. [8–13], although precursors considering excited atoms go back further (e.g. Refs. [14–16]). The theories for different non-equilibrium situations, albeit apparently disparate, may be shown to concord as they should [17].

In the following we consider a particle prepared in an energy eigenstate $|n\rangle$ placed in an environment of macroscopic bodies at uniform temperature T, the situation originally considered in Ref. [12]. The CP potential of the particle may be written as

$$U_n = \sum_k U_{nk} \tag{1.1}$$

where the sum runs over all other eigenstates $|k\rangle$ to which there is an allowed dipole transition. Both for cold molecules [18] and Rydberg atoms [19] it was found that although the number of states $|k\rangle$ to be summed over in Eq. (1.1) is formally infinite, only a few transitions give significant contributions. To wit, the important transitions were found to be those corresponding to the smallest difference in eigenenergy $\Delta E_{kn} = E_k - E_n$, i.e. the smallest transition frequency $\omega_{kn} = \Delta E_{kn}/\hbar$ or correspondingly the longest transition wavelength $\lambda_{kn} = 2\pi c/\omega_{kn}$. Because of this fact the typical values of λ_{kn} for cold polar molecules and Rydberg atoms alike are usually much larger than the typical distance z from the particle to a nearby body in experiments involving surfaces. In other words, for the dominating transitions $|n\rangle \to |k\rangle$,

$$\frac{z}{\lambda_{kn}} = \frac{\omega_{kn} z}{2\pi c} \gg 1, \tag{1.2}$$

so the interaction is essentially *non-retarded*.

Recently, it was found that in the non-retarded regime the CP interaction near a metallic half-space is virtually temperature independent[20]. The thermal CP potential then agrees with its zero-temperature counterpart for all temperatures. This was later shown to be a reasonable approximation for bodies of arbitrary shape [21]. Temperature-dependent corrections to the zero-temperature potential were identified to stem from retardation and imperfect conductivity. The magnitude of the latter corrections were found to strongly depend on the body shape and curvature, demonstrating that geometry and temperature are closely intertwined [22].

In the present paper we study these corrections in detail for an atom interacting with a metal sphere, being a prototype of a body with a curved surface. Various embodiments of the particle–sphere interactions at zero temperature have been treated by a number of authors [23–30]. We study the linear temperature-dependent correction in the spectroscopic high-temperature regime

$$k_{\mathrm{B}} T \gg \hbar\omega_{kn}, \tag{1.3}$$

and for nonretarded distances. We quote here the final result, to be derived below, for the thermal Casimir-Polder potential of an atom at distance r from the center of a metal sphere of radius R:

$$U_{nk}(r) = -\frac{|\mathbf{d}_{kn}|^2}{24\pi\varepsilon_0 r^3}\frac{\phi^3(6-3\phi^2+\phi^4)}{(1-\phi^2)^3} + \frac{|\mathbf{d}_{kn}|^2}{24\pi\varepsilon_0 r^3}\left(\frac{k_{\rm B}T}{\hbar\omega_{kn}}-\frac{1}{2}\right)\Big\{x^2\big[3(1+3\phi^4)\mathrm{artanh}\phi - \phi(3-\phi^2) + 2\phi^3\log(1-\phi^2)\big] + 2x\phi^2\mathrm{Re}\Big\{\frac{i}{\sqrt{\varepsilon(\omega)}}\Big\}\Big[\frac{3+7\phi^2-4\phi^4}{(1-\phi^2)^2} - \log(1-\phi^2)\Big] + ...\Big\} + \mathcal{O}(T^{-1}) \tag{1.4}$$

where we have introduced the dimensionless distance

$$x = \frac{r\omega_{kn}}{c} \tag{1.5}$$

and a geometry parameter

$$\phi = R/r. \tag{1.6}$$

The expression (1.4) holds when $x \ll 1$, but $\mathrm{Im}\{\sqrt{\varepsilon}\}x\phi = \mathrm{Im}\{\sqrt{\varepsilon}\}\omega_{kn}R/c$ still significantly exceeds unity. The dots indicate higher-order contributions in the small parameters x and $1/(x\sqrt{\varepsilon})$. For definitions of the various quantities in Eq. (1.4), see Sec. II below.

II. GENERAL FORMALISM

The general formalism for the temperature-dependent CP force on a particle in an energy eigenstate is found in Ref. [12]. Here we shall restrict our attention to the special case of an isotropic particle, and consider a single transition $|n\rangle \to |k\rangle$ so that the particle can be treated as an effective two-level system. The generalisation to anisotropic particles (c.f. Ref. [12]), and inclusion of more levels can be achieved immediately by summing up contributions from several dipole transitions according to Eq. (1.1). For a cold polar molecule or a Rydberg atom only a small number of transitions are of significance, and these all have transition wavelengths of the same order of magnitude. Our considerations for a single transition will then hold for all significant transitions.

This section reviews the general framework for treating the small temperature correction in the non-resonant regime for arbitrary geometries, which we apply below to a metal sphere. In the notation of Ref. [21], the CP potential of an isotropic non-magnetic particle in state $|n\rangle$ due to a possible transition to state $|k\rangle$ splits naturally into a non-resonant (nr) and a resonant (r) part [12]

$$U_{nk}(\mathbf{r}) = U^{\rm nr}_{nk}(\mathbf{r}) + U^{\rm r}_{nk}(\mathbf{r}), \tag{2.1}$$

where the two parts are given by

$$U^{\rm nr}_{nk}(\mathbf{r}) = -\frac{2k_{\rm B}T|\mathbf{d}_{nk}|^2\omega_{kn}}{3\hbar\varepsilon_0}{\sum_{j=0}^{\infty}}' \frac{\Gamma_{{\rm i}\xi_j}(\mathbf{r})}{\omega_{kn}^2+\xi_j^2}; \tag{2.2a}$$

$$U^{\rm r}_{nk}(\mathbf{r}) = \frac{|\mathbf{d}_{kn}|^2}{3\varepsilon_0}\, n(\omega_{kn})\mathrm{Re}\,\Gamma_{\omega_{kn}}(\mathbf{r}). \tag{2.2b}$$

Here, $\mathbf{d}_{kn} = \langle k|\mathbf{d}|n\rangle$ is the transition dipole matrix element and

$$\xi_j = 2\pi j k_{\rm B}T/\hbar \tag{2.3}$$

are the Matsubara frequencies. The photon number at frequency ω and temperature T is given by the Bose-Einstein distribution,

$$n(\omega) = \frac{1}{\exp(\hbar\omega/k_{\rm B}T)-1} = -[n(-\omega)+1]. \tag{2.4}$$

The function

$$\Gamma_\omega(\mathbf{r}) \equiv \frac{\omega^2}{c^2}\lim_{\mathbf{r}'\to\mathbf{r}}\mathrm{tr}\mathbf{G}^{(1)}(\mathbf{r},\mathbf{r}',\omega) \tag{2.5}$$

is given in terms of the scattering part $\mathbf{G}^{(1)}$ of the total dyadic Green's function satisfying

$$\left[\nabla\times\nabla\times\ -\frac{\omega^2}{c^2}\varepsilon(\mathbf{r},\omega)\right]\mathbf{G}(\mathbf{r},\mathbf{r}',\omega) = \delta(\mathbf{r}-\mathbf{r}')\mathbf{1}. \tag{2.6}$$

($\mathbf{1}$: unit tensor). The relative permittivity $\varepsilon(\mathbf{r},\omega)$ of the present bodies is isotropic and we have assumed the bodies to be non-magnetic. Due to causality, $\Gamma_{{\rm i}\xi_j}$ is real, being a generalized susceptibility evaluated at imaginary frequency, so in particular $\Gamma_{{\rm i}0} = \Gamma_0$ is real.

In the following, we consider a single transition $|n\rangle \to |k\rangle$ and simplify our notation according to

$$|\mathbf{d}_{kn}|^2 \to |\mathbf{d}|^2;\ \ \omega_{kn}\to\omega;\ \ U_{nk}(\mathbf{r})\to U(\mathbf{r}).$$

Note that ω can be either positive or negative depending on whether the transition is upwards or downwards.

We concentrate on the spectroscopic high-temperature regime, Eq. (1.3), in which one easily verifies that the contribution of the lowest Matsbubara frequency ($j=0$) dominates in Eq. (2.2a),

$$U^{\rm nr}(\mathbf{r}) = -\frac{|\mathbf{d}|^2}{3\varepsilon_0}\frac{k_{\rm B}T}{\hbar\omega}\Gamma_0(\mathbf{r}) + \mathcal{O}(T^{-1}). \tag{2.7}$$

The photon number in this regime is

$$n(\omega) = \frac{k_{\rm B}T}{\hbar\omega} - \frac{1}{2} + \mathcal{O}(T^{-1}), \tag{2.8}$$

so the resonant potential (2.2b) reads

$$U^{\rm r}(\mathbf{r}) = \frac{|\mathbf{d}|^2}{3\varepsilon_0}\left(\frac{k_{\rm B}T}{\hbar\omega}-\frac{1}{2}\right)\mathrm{Re}\Gamma_\omega(\mathbf{r}). \tag{2.9}$$

Combining these results, we find for the full potential in the spectroscopic high-temperature regime,

$$U(\mathbf{r}) = -\frac{|\mathbf{d}|^2}{6\varepsilon_0}\Gamma_0(\mathbf{r}) + \frac{|\mathbf{d}|^2}{3\varepsilon_0}\left(\frac{k_{\rm B}T}{\hbar\omega}-\frac{1}{2}\right)\mathrm{Re}\Delta\Gamma_\omega(\mathbf{r}) + \mathcal{O}(T^{-1}) \tag{2.10}$$

where $\Delta\Gamma_\omega = \Gamma_\omega - \Gamma_0$.

For comparison, in the zero-temperature limit, in which the Matsubara sum becomes an integral according to standard procedures (e.g. the Euler-Maclaurin formula), one obtains

$$U(\mathbf{r})\big|_{T=0} = -\frac{|\mathbf{d}|^2\omega}{3\pi\varepsilon_0}\int_0^\infty \mathrm{d}\xi \frac{\mathrm{tr}\Gamma^{(1)}_{\mathrm{i}\xi}(\mathbf{r})}{\omega^2+\xi^2} - \frac{|\mathbf{d}|^2}{3\varepsilon_0}\Theta(\omega)\mathrm{Re}\,\Gamma_\omega(\mathbf{r}) \tag{2.11}$$

with $\Theta(x)$ denoting the unit step function.

In the nonretarded and perfect-conductor limits, we have $\Gamma_{\mathrm{i}\xi}(\mathbf{r}) \simeq \mathrm{Re}\Gamma_\omega(\mathbf{r}) \simeq \Gamma_0(\mathbf{r})$ [20] which implies $\mathrm{Re}\Delta\Gamma_\omega(\mathbf{r}) \simeq 0$. In this case, both Eqs. (2.10) and (2.11) reduce to

$$U_0(\mathbf{r}) = -\frac{|\mathbf{d}|^2}{6\varepsilon_0}\Gamma_0(\mathbf{r}) \tag{2.12}$$

and the CP potential is independent of temperature throughout.

In this article, we are interested in the corrections to the temperature-independent result (2.12) that arise due to small violations of the non-retarded limit and perfect reflectivity. As seen from Eq. (2.10), they are governed by $\mathrm{Re}\Delta\Gamma_\omega(\mathbf{r})$. When all present macroscopic bodies are perfectly conducting (PC), then Γ_ω satisfies [21]

$$\Gamma^{\mathrm{PC}}_\omega = \Gamma^{\mathrm{PC}}_0 + \frac{\omega^2}{2c^2}\frac{\mathrm{d}^2\Gamma^{\mathrm{PC}}_\omega}{\mathrm{d}\omega^2}\Big|_{\omega=0} + \ldots\,; \quad \omega\to 0, \tag{2.13}$$

so that

$$\Delta\Gamma^{\mathrm{PC}}_\omega \approx \frac{\omega^2}{2c^2}\frac{\mathrm{d}^2\Gamma^{\mathrm{PC}}_\omega}{\mathrm{d}\omega^2}\Big|_{\omega=0}; \quad \omega\to 0, \tag{2.14}$$

is quadratic in ω. This correction accounts for the fact that electromagnetic interactions are transmitted at the finite speed of light; we will refer to it as the retardation correction in the following.

For an imperfect conductor, the corrections to the Green's function for small frequencies includes a second correction due to the frequency-dependence of the reflectivity of the bodies. We write

$$\Delta\Gamma_\omega = \Delta\Gamma^{\mathrm{ret.}}_\omega + \Delta\Gamma^{\mathrm{refl.}}_\omega \tag{2.15}$$

due to retardation and reflectivity, respectively. When treating ω and $\varepsilon(\omega)$ as independent variables, the retardation correction $\Delta\Gamma^{\mathrm{ret.}}_\omega$ is the leading-order term in $1/\sqrt{\varepsilon(\omega)}$ and next-to-leading in ω; whereas the reflectivity correction $\Delta\Gamma^{\mathrm{refl.}}_\omega$ is the contribution sub-leading in $1/\sqrt{\varepsilon(\omega)}$ and leading in ω. Note that the perfect-conductor limit $\varepsilon(\omega)\to\infty$ does not commute with the nonretarded limit $\omega\to 0$ in this case. The incompatibility of the two limits was first pointed out in Ref. [31] and is at the heart of the debate over the temperature correction to the Casimir effect [32]. For a metal body at typical frequencies and distances, the perfect-conductor limit has to be performed before the nonretarded limit, see Sect. III below.

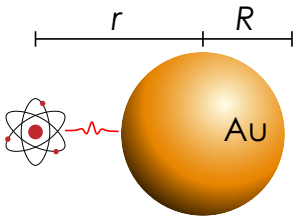

FIG. 1: The geometry considered: a quantum particle prepared in eigenstate $|n\rangle$ outside a gold sphere.

With the leading corrections to the Green's function being given by Eq. (2.15), the thermal CP potential (2.12) can be given as

$$U(\mathbf{r}) = U_0(\mathbf{r}) + \Delta U_{\mathrm{ret.}}(\mathbf{r}) + \Delta U_{\mathrm{refl.}}(\mathbf{r}) + \mathcal{O}(T^{-1}) \tag{2.16}$$

with

$$\Delta U_i(\mathbf{r}) = \frac{|\mathbf{d}|^2}{3\varepsilon_0}\left(\frac{k_{\mathrm{B}}T}{\hbar\omega}-\frac{1}{2}\right)\mathrm{Re}\Delta\Gamma^i_\omega(\mathbf{r}), \tag{2.17}$$

$i = \mathrm{ret.}, \mathrm{refl.}$ The relative corrections due to retardation and reflection read

$$\frac{\Delta U_i(\mathbf{r})}{U_0(\mathbf{r})} = -2\left(\frac{k_{\mathrm{B}}T}{\hbar\omega}-\frac{1}{2}\right)\frac{\mathrm{Re}\Delta\Gamma^i_\omega(\mathbf{r})}{\Gamma_0(\mathbf{r})}\,. \tag{2.18}$$

Note that $\mathrm{Re}\Delta\Gamma_\omega(\mathbf{r})$ is an even function of ω, as follows directly from definition (2.5) together with the Schwarz reflection principle $\mathbf{G}(\mathbf{r},\mathbf{r}';-\omega) = \mathbf{G}^*(\mathbf{r},\mathbf{r}';\omega)$. As a consequence, the leading temperature corrections in the high-temperature limit, being proportional to $\mathrm{Re}\Delta\Gamma_\omega(\mathbf{r})/\omega$, change sign when comparing downward and upward transitions.

III. CASIMIER–POLDER POTENTIAL NEAR A SPHERE

As depicted in Fig. 1, we consider a particle at distance r from the center of a sphere of radius R and permittivity $\varepsilon = \varepsilon(\omega)$. The dyadic Green's function leads to [28]

$$\Gamma_\omega(\mathbf{r}) = \frac{ix}{4\pi r^3}\sum_{l=1}^\infty (2l+1)\Big\{x^2 r_l^{\mathrm{TE}}(\phi x)h_l^{(1)}(x)^2 + r_l^{\mathrm{TM}}(\phi x)\Big[l(l+1)h_l^{(1)}(x)^2 + \tilde{h}_l^{(1)\prime}(x)^2\Big]\Big\} \tag{3.1}$$

where $h_l^{(1)}(x)$ is the spherical Hankel function of the first kind, $\tilde{h}_l^{(1)\prime}(x)$ [and for future reference, $\tilde{\jmath}_l'(x)$] is shorthand for

$$\tilde{h}_l^{(1)\prime}(x) = [xh_l^{(1)}(x)]'; \quad \tilde{\jmath}_l'(x) = [xj_l(x)]' \tag{3.2}$$

[$j_l(x)$: spherical Bessel function of the first kind]. For convenience we are using the dimensionless distance and

size parameters $x = r\omega/c$ and $0 < \phi = R/r < 1$, recall Eqs. (1.5) and (1.6). The reflection coefficients for TE and TM-polarized waves read

$$r_l^{\rm TE}(z) = -\frac{\tilde{j}_l'(z) j_l(\sqrt{\varepsilon}z) - \tilde{j}_l'(\sqrt{\varepsilon}z) j_l(z)}{\tilde{h}_l^{(1)\prime}(z) j_l(\sqrt{\varepsilon}z) - \tilde{j}_l'(\sqrt{\varepsilon}z) h_l^{(1)}(z)}; \quad (3.3a)$$

$$r_l^{\rm TM}(z) = -\frac{\varepsilon\tilde{j}_l'(z) j_l(\sqrt{\varepsilon}z) - \tilde{j}_l'(\sqrt{\varepsilon}z) j_l(z)}{\varepsilon\tilde{h}_l^{(1)\prime}(z) j_l(\sqrt{\varepsilon}z) - \tilde{j}_l'(\sqrt{\varepsilon}z) h_l^{(1)}(z)}. \quad (3.3b)$$

In the following we assume both the particle–center separation and the sphere size to be non-retarded, $\phi x \leq x \ll 1$. In addition, we perform the perfect-conductor limit $|\varepsilon| \gg 1$. To leading order, the two limits commute: Taking the perfect-conductor limit first, the reflection coefficients reduce to

$$r_l^{\rm TE}(\phi x) \overset{\varepsilon\to\infty}{\longrightarrow} r_l^{\rm TE,PC}(\phi x) = -\frac{j_l(\phi x)}{h_l^{(1)}(\phi x)}; \quad (3.4)$$

$$r_l^{\rm TM}(\phi x) \overset{\varepsilon\to\infty}{\longrightarrow} r_l^{\rm TM,PC}(\phi x) = -\frac{\tilde{j}_l'(\phi x)}{\tilde{h}_l^{(1)\prime}(\phi x)}, \quad (3.5)$$

see the asymptotes (A1) and (A2) in App. A. Using the expansions (A3) and (A4), they further simplify to

$$r_l^{\rm TE,PC}(\phi x) \overset{\phi x\to 0}{\longrightarrow} r_{l,0}^{\rm TE,PC}(\phi x) = -\frac{{\rm i}(\phi x)^{2l+1}}{(2l+1)!!(2l-1)!!}; \quad (3.6)$$

$$r_l^{\rm TM,PC}(\phi x) \overset{\phi x\to 0}{\longrightarrow} r_{l,0}^{\rm TM,PC}(\phi x) = \frac{l+1}{l}\frac{{\rm i}(\phi x)^{2l+1}}{(2l+1)!!(2l-1)!!} \quad (3.7)$$

in the non-retarded limit. Here, $(2l+1)!! = 1\cdot 3\cdots(2l+1)$.

In contrast, when taking the non-retarded limit first, one finds

$$r_l^{\rm TE}(\phi x) \overset{\phi x\to 0}{\longrightarrow} r_{l,0}^{\rm TE}(\phi x) = (\varepsilon-1)\frac{{\rm i}(\phi x)^{2l+3}}{(2l+3)!!(2l+1)!!}; \quad (3.8)$$

$$r_l^{\rm TM}(\phi x) \overset{\phi x\to 0}{\longrightarrow} r_{l,0}^{\rm TM}(\phi x) = \frac{(l+1)(\varepsilon-1){\rm i}(\phi x)^{2l+1}}{(l\varepsilon+l+1)(2l+1)!!(2l-1)!!}, \quad (3.9)$$

and subsequently

$$r_{l,0}^{\rm TE}(\phi x) \overset{\varepsilon\to\infty}{\longrightarrow} \varepsilon\frac{{\rm i}(\phi x)^{2l+3}}{(2l+3)!!(2l+1)!!}; \quad (3.10)$$

$$r_{l,0}^{\rm TM}(\phi x) \overset{\varepsilon\to\infty}{\longrightarrow} \frac{l+1}{l}\frac{{\rm i}(\phi x)^{2l+1}}{(2l+1)!!(2l-1)!!}. \quad (3.11)$$

While the TM-coefficient takes the same form regardless of the order of the limits, the TE-coefficient yields different results, depending on which of the two limits is performed first.

However, the Green tensor in the non-retarded limit is dominated by $r_l^{\rm TM}$. Substituting the results for the reflection coefficients into (3.1), using the approximation (A4) from App. A and retaining only the leading order in x, one finds

$$\begin{aligned}\Gamma_0^{\rm PC}(\mathbf{r}) =& \frac{1}{4\pi r^3}\sum_{l=1}^{\infty}(2l+1)(l+1)\phi^{2l+1} \\ =& \frac{1}{4\pi r^3}\frac{\phi^3(6-3\phi^2+\phi^4)}{(1-\phi^2)^3}. \end{aligned} \quad (3.12)$$

With this result, the temperature-invariant CP potential (2.12) reads

$$U_0(\mathbf{r}) = -\frac{|\mathbf{d}|^2}{24\pi\varepsilon_0 r^3} f(\phi) \quad (3.13)$$

with

$$f(\phi) = \frac{\phi^3(6-3\phi^2+\phi^4)}{(1-\phi^2)^3} \to \begin{cases} 6\phi^3 & \text{for } \phi\to 0, \\ \dfrac{1}{2(1-\phi)^3} & \text{for } \phi\to 1. \end{cases} \quad (3.14)$$

This is in agreement with the zero-temperature potential as found in Ref. [29] for a perfectly conducting sphere in the non-retarded limit on the basis of image-charge techniques. As discussed in Ref. [33], the atom-sphere geometry is a particular example of a two-parameter geometry, conveniently described by a scaling function $f(\phi)$.

The accuracy of the temperature-independent result is demonstrated numerically in Fig. 2 for a ground-state two-level particle outside a gold sphere. The permittivity of the sphere has been described by a Drude model $\varepsilon(\omega) = 1-\omega_P^2/[\omega(\omega+i\gamma)]$ with parameters $\omega_P = 9$eV and $\gamma = 35$meV. For comparison, the same situation but with a smaller sphere is shown in Fig. 3. We see that Eq. (3.13) yields a very good approximation. The exact potential is slightly smaller by at most 5% for $r\omega/c = 0.1$. Recall that the leading correction in the high-temperature limit has opposite signs for ground-state and excited atoms. For an excited two-level atom, we would hence find that the exact potential is slightly larger than its approximation (3.13). In the following, we derive analytical expressions for the leading temperature-dependent corrections to Eq. (3.13).

A. Correction from retardation

When considering the full thermal CP potential (3.13), the non-retarded and perfect-conductor limits do not commute. We have $\phi x \leq x \ll 1$ and $|\varepsilon| \gg 1$, which is compatible with both large and small values of $|\sqrt{\varepsilon}|\phi x$. For a metal sphere at typical experimental distances of order micrometers and $x \sim 0.01 - 0.001$, we have ${\rm Im}\sqrt{\varepsilon}\phi x \gg 1$, meaning that the perfect-conductor limit has to be applied first. The opposite limit $|\sqrt{\varepsilon}|\phi x \ll 1$ may be realised for some dielectrics with large electrostatic permittivity, in which case the nonretarded limit would have to be performed first.

The correction from retardation effects is found by using the perfect conductor values (3.4) and (3.5) of the

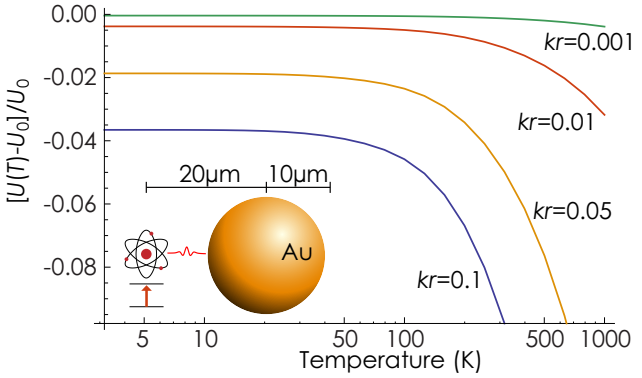

FIG. 2: Numerical comparison of the exact CP potential $U(T)$ of a two-level model particle (transition energy $\hbar ck$) outside a gold sphere with the T-independent result U_0 for a perfect conductor in the non-retarded limit. Parameter values: $R = \frac{1}{2}r = 10\mu$m.

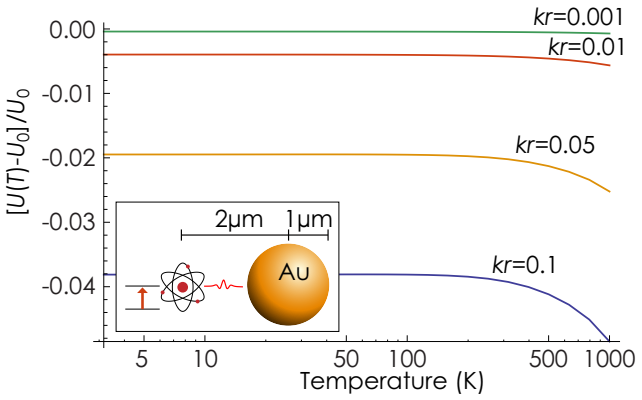

FIG. 3: Same as figure 2, but with a smaller gold sphere: $R = \frac{1}{2}r = 1\mu$m.

reflection coefficients and expanding $\Gamma_\omega^{\rm PC}(\mathbf{r})$ as given by Eq. (3.1) in powers of x, the leading correction term being of order x^2. We obtain such quadratic corrections from three sources: (A) from the TM-mode reflection coefficient $r_l^{\rm TM,PC}$; (B) from TM-mode propagators $h_l^{(1)}(x)^2$ and $\tilde{h}_l^{(1)\prime}(x)^2$; and (C) from the leading-order TE-mode contribution. The technical details of the small x expansions of the different cases are found in App.A 1.

As shown therein, correction (A) takes the form

$$r_l^{\rm TM,PC}(\phi x) = r_{l,0}^{\rm TM,PC}(\phi x)\left\{1-\frac{(\phi x)^2}{2}\left[\frac{l+3}{(2l+3)(l+1)}+\frac{l-2}{l(2l-1)}\right]+...\right\} \tag{3.15}$$

with $r_{l,0}^{\rm TM,PC}$ being given by Eq. (3.7). The correction (B) is found to be

$$r_{l,0}^{\rm TM,PC}(\phi x)\left[l(l+1)h_l^{(1)}(x)^2+\tilde{h}_l^{(1)\prime}(x)^2\right] = \frac{(l+1)\phi^{2l+1}}{ix}\left[1+\frac{x^2}{2l+1}+...\right]. \tag{3.16}$$

Finally, the correction (C) from the TE-mode takes the simple form

$$r_l^{\rm TE,PC}(\phi x)h_l^{(1)}(x)^2 = -\frac{\phi^{2l+1}}{ix(2l+1)}+... \tag{3.17}$$

Substituting these corrections into Eq. (3.1), one finds

$$\Delta\Gamma_\omega^{\rm ret.} = \frac{x^2}{4\pi r^3}\sum_{l=1}^{\infty}\left\{l\phi^{2l+1}-(2l+1)\left[\frac{l+3}{2l+3}+\frac{(l+1)(l-2)}{(2l-1)l}\right]\frac{\phi^{2l+3}}{2}\right\} \tag{3.18}$$

The sum may be carried out in closed form by splitting the expressions into partial fractions. One finds

$$\Delta\Gamma_\omega^{\rm ret.} = \frac{x^2}{8\pi r^3}\left[3(1+3\phi^4)\text{artanh}\phi-\phi(3-\phi^2)+2\phi^3\log(1-\phi^2)\right]. \tag{3.19}$$

Substituting this result into Eq. (2.17), we obtain the retardation correction

$$\Delta U_{\rm ret.}(\mathbf{r}) = \frac{|\mathbf{d}|^2x^2}{24\pi\varepsilon_0 r^3}\left(\frac{k_{\rm B}T}{\hbar\omega}-\frac{1}{2}\right)g_{\rm ret.}(\phi) \tag{3.20}$$

with scaling function

$$g_{\rm ret.}(\phi) = 3(1+3\phi^4)\text{artanh}\phi-\phi(3-\phi^2)+2\phi^3\log(1-\phi^2) \to \begin{cases}2\phi^3 & \text{for } \phi\to 0,\\ -4\log(1-\phi) & \text{for } \phi\to 1.\end{cases} \tag{3.21}$$

Its relative contribution (2.18) is given by

$$\frac{\Delta U_{\rm ret.}(\mathbf{r})}{U_0(\mathbf{r})} = -\left(\frac{k_{\rm B}T}{\hbar\omega}-\frac{1}{2}\right)x^2\,\frac{g_{\rm ret.}(\phi)}{f(\phi)}. \tag{3.22}$$

B. Correction from imperfect reflection

The leading order corrections to the ideal reflection coefficients are calculated in App. A 2 and have the form

$$r_l^{\rm TE}(\phi x) = r_{l,0}^{\rm TE,PC}(\phi x)\left[1-\frac{i(2l+1)}{\sqrt{\varepsilon}\phi x}+...\right]; \tag{3.23a}$$

$$r_l^{\rm TM}(\phi x) = r_{l,0}^{\rm TM,PC}(\phi x)\left[1+\frac{i\phi x}{\sqrt{\varepsilon}}\,\frac{2l+1}{l(l+1)}+...\right] \tag{3.23b}$$

for $x \ll 1$, with $r_{l,0}^{\mathrm{TE,PC}}$ and $r_{l,0}^{\mathrm{TM,PC}}$ given by Eqs. (3.6) and (3.7). Substituting these results into Eq. (3.1) and using the leading-order small argument expansions in Eqs. (3.16) and (3.17), we find

$$\Delta\Gamma_{\omega}^{\mathrm{refl.}} = \frac{ix}{4\pi r^3\sqrt{\varepsilon}} \sum_{l=1}^{\infty} (2l+1) \left[1 + \frac{2l+1}{l}\phi^2\right] \phi^{2l}$$
$$= \frac{ix\phi^2}{4\pi r^3\sqrt{\varepsilon}} \left[\frac{3+7\phi^2-4\phi^4}{(1-\phi^2)^2} - \log(1-\phi^2)\right]. \qquad (3.24)$$

Inserting this into Eq. (2.17), the reflectivity correction is found to be

$$\Delta U_{\mathrm{refl.}}(\mathbf{r}) = \frac{|\mathbf{d}|^2 x}{24\pi\varepsilon_0 r^3} \mathrm{Re}\left(\frac{\mathrm{i}}{\sqrt{\varepsilon}}\right) \left(\frac{k_{\mathrm{B}}T}{\hbar\omega} - \frac{1}{2}\right) g_{\mathrm{refl.}}(\phi) \qquad (3.25)$$

with scaling function

$$g_{\mathrm{refl.}}(\phi) = 2\phi^2 \left[\frac{3+7\phi^2-4\phi^4}{(1-\phi^2)^2} - \log(1-\phi^2)\right]$$
$$\to \begin{cases} 6\phi^2 & \text{for } \phi \to 0, \\ \dfrac{3}{(1-\phi)^2} & \text{for } \phi \to 1. \end{cases} \qquad (3.26)$$

Its relative contribution (2.18) reads

$$\frac{\Delta U_{\mathrm{refl.}}(\mathbf{r})}{U_0(\mathbf{r})} = -\left(\frac{k_{\mathrm{B}}T}{\hbar\omega} - \frac{1}{2}\right) x \mathrm{Re}\left(\frac{\mathrm{i}}{\sqrt{\varepsilon}}\right) \frac{g_{\mathrm{refl.}}(\phi)}{f(\phi)}. \qquad (3.27)$$

C. Discussion and comparison

Combining the T-invariant result (2.12) with the retardation and reflectivity corrections (3.20) and (3.25), we obtain the weakly temperature-dependent CP potential (1.4), as stated in the introduction. The quality of this analytic high-temperature result is demonstrated in Fig. 4 where we compare it with the result of a numerical simulation for a ground-state two-level particle outside a gold sphere. One sees that the analytic result is an excellent approximation for temperatures $T > 200\,\mathrm{K}$. Recall from Fig. 2 that this is the range where deviations from the temperature-independent result (2.12) exceed the 0.5% level and start becoming noticeable.

According to Eqs. (3.22) and (3.27), the relative contributions from retardation and finite reflectivity are governed by the ratios $g_i(\phi)/f(\phi)$ of the scaling functions as given by Eqs. (3.14),(3.21) and (3.26). These ratios are depicted in Fig. 5. The figure shows that both contributions strongly depend on the curvature of the sphere as parametrised by ϕ. The retardation contribution takes a value 1/3 for a strongly curved sphere and stays approximately constant for $\phi \lesssim 0.5$. In the limit of a flat surface, it rapidly falls off as $-4(1-\phi)^3\log(1-\phi)$. The reflectivity correction grows as $1/\phi$ in the limit of a strongly curved sphere and falls off gently as $6(1-\phi)$ in the limit of a flat surface.

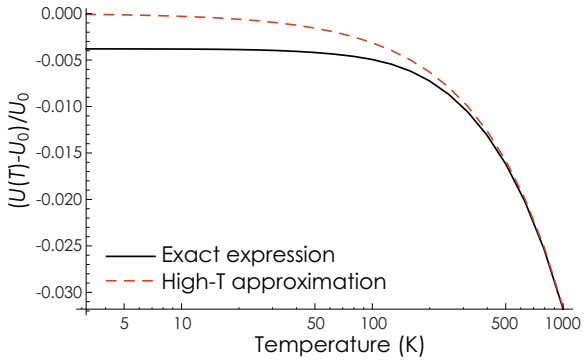

FIG. 4: Comparison of the exact temperature-correction to the CP potential to the of a two-level model particle (transition energy $\hbar ck$) outside a gold sphere with the analytical high-temperature approximation. Parameters are $r = 2R = 20\mu$m, $x = \omega r/c = 0.01$.

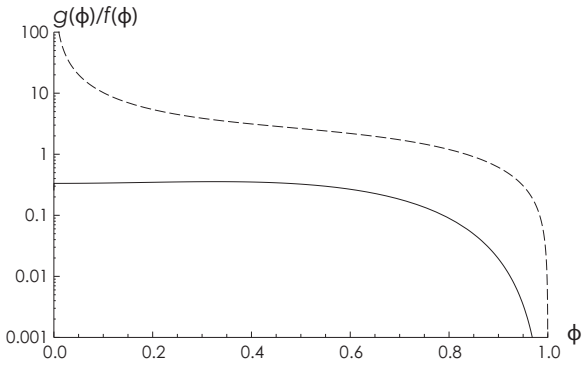

FIG. 5: Ratios of the scaling functions $g_{\mathrm{ret.}}(\phi)/f(\phi)$ (solid line) and $g_{\mathrm{refl.}}(\phi)/f(\phi)$ (dashed line) that govern the impact of retardation and finite reflectivity on the thermal CP potential.

The ratio $g_{\mathrm{refl.}}(\phi)/f(\phi)$ is greater than $g_{\mathrm{ret.}}(\phi)/f(\phi)$ by at least an order of magnitude for all curvatures. One has to bear in mind, however, that the reflectivity correction carries an additional factor $\mathrm{Re}(\mathrm{i}/\sqrt{\varepsilon})/x \ll 1$. For a metal described by a Drude model with $\omega, \gamma \ll \omega_P$, one finds

$$\mathrm{Re}\left[\mathrm{i}/\sqrt{\varepsilon(\omega)}\right] = \omega_P^{-1} \left[\tfrac{1}{2}(\sqrt{\omega^2+\gamma^2} + |\omega|)|\omega|\right]^{\frac{1}{2}}$$
$$\simeq \begin{cases} \sqrt{\omega\gamma/2}/\omega_P & \text{for } \omega \ll \gamma, \\ \omega/\omega_P & \text{for } \omega \gg \gamma. \end{cases} \qquad (3.28)$$

Depending on the actual value of $\mathrm{Re}(\mathrm{i}/\sqrt{\varepsilon})/x \ll 1$ for a given molecule and material, either one of the reflectivity or retardation may dominate for given curvatures. However, the asymptotic behaviour observed in Fig. 5 shows that the reflectivity correction will always dominate in the limits of small or large curvature.

IV. SUMMARY

In recent publications it has been shown that the Casimir–Polder potential acting on a particle prepared in an eigenstate at a non-retarded distance from a macroscopic body can be virtually independent of the surrounding temperature. It has been shown that this feature is not a property of simple planar geometry, but applies to bodies of arbitrary shape, when these are perfectly conducting, or to many geometries when they are described by more realistic metallic permittivity models. weakly temperature-dependent corrections to the potential of a metal body have been identified to stem from retardation and imperfect reflectivity.

In the present paper, we have studied the weakly temperature-dependent CP potential of a particle near a metal sphere. We have assumed both the particle–sphere distance and the particle's transition frequency to be small enough so that retardation and imperfect reflectivity present only small perturbations to the temperature-independent result. Such is typically the case in experimental set-ups in which cold polar molecules or Rydberg atoms are used, whose interaction potential is dominated by long wavelength transitions for which the non-retarded regime extends to tens and hundreds of micrometers, respectively. A numerical study has shown that the temperature-independent potential may underestimate the exact thermal result for a ground-state particle by about 5%.

In addition, we have obtained analytic expressions for the perturbative retardation and reflectivity corrections. Our results show that reflectivity is the dominant correction for very large or small curvatures, while intermediate curvatures may be governed by either retardation and reflectivity corrections, depending on particle and material. Our analytic result provides a description of the weakly temperature-dependent CP potential of a particle near a metal sphere at non-retarded distances that is faithful to about 0.5%.

We thank Ho Trung Dung for discussions. This work was supported by the UK Engineering and Physical Sciences Research Council. Support from the European Science Foundation (ESF) within the activity 'New Trends and Applications of the Casimir Effect' is gratefully acknowledged.

Appendix A: Limits and their leading corrections

To calculate the CP potential in the perfect-conductor and non-retarded limits, we need to approximate the spherical Bessel functions for small and large arguments. Using the asymptotes from §10 of Ref. [34]

$$j_l(x) \approx \frac{\sin(x - l\pi/2)}{x} \quad \text{for } x \gg 1; \tag{A1}$$

$$h_l^{(1)}(x) \approx \frac{(-\mathrm{i})^{l+1}\mathrm{e}^{\mathrm{i}(x-n\pi/2)}}{x} \quad \text{for } x \gg 1, \tag{A2}$$

we easily find the perfect-conductor limits (3.4) and (3.5).

The non-retarded limits (3.6), (3.7), (3.8) and (3.9) can be found by using the expansions [34]

$$j_l(x) = \frac{x^l}{(2l+1)!!} - \frac{x^{l+2}}{2(2l+3)!!} + \ldots \quad \text{for } x \ll 1; \tag{A3}$$

$$h_l^{(1)}(x) = -\frac{\mathrm{i}(2l-1)!!}{x^{l+1}} - \frac{\mathrm{i}(2l-3)!!}{2x^{l-1}} + \ldots \quad \text{for } x \ll 1 \tag{A4}$$

with $(2l+1)!! = 1\cdot 3\cdot 5\cdots(2l+1)$. Note that the next-to-leading order expansion is only needed for (3.8), where the leading-order term vanishes.

1. Retardation corrections

To calculate the retardation correction to the perfect-conductor TM-mode reflection coefficients (3.5), we use the expansions (A3) and (A4), which together with the definitions (3.2) lead to

$$\tilde{j}_l'(x) = \frac{(l+1)x^l}{(2l+1)!!}\left[1 - \frac{x^2}{2}\frac{l+3}{(2l+3)(l+1)} + \ldots\right] \tag{A5a}$$

$$\tilde{h}_l^{(1)\prime}(x) = \frac{il(2l-1)!!}{x^{l+1}}\left[1 + \frac{x^2}{2}\frac{l-2}{l(2l-1)} + \ldots\right] \tag{A5b}$$

for $x \ll 1$. This immediately yields Eq. (3.15).

The retardation correction from the propagator factors are found from expansions

$$h_l^{(1)}(x)^2 = -\frac{[(2l-1)!!]^2}{x^{2l+2}}\left[1 + \frac{x^2}{2l-1} + \ldots\right]; \tag{A6a}$$

$$\tilde{h}_l^{(1)\prime}(x)^2 = -\frac{l^2[(2l-1)!!]^2}{x^{2l+2}}\left[1 + \frac{x^2(l-2)}{l(2l-1)} + \ldots\right] \tag{A6b}$$

which follow from Eqs. (A4) and (A5b). Combining these results with $r_{l,0}^{\mathrm{TM,PC}}$ as given by Eq. (3.7), we arrive at Eq. (3.16).

Expansion (A6a) moreover combines with $r_{l,0}^{\mathrm{TE,PC}}$ as given by Eq. (3.6) to result in Eq. (3.17).

2. Finite reflectivity correction

In order to expand the reflection coefficients (3.3) in powers of ε^{-1}, we rewrite them as

$$r_l^{\mathrm{TM}}(\phi x) = r_l^{\mathrm{TM,PC}}(\phi x)\frac{1 - AJ/\varepsilon}{1 - AH/\varepsilon};$$

$$r_l^{\mathrm{TE}}(\phi x) = r_l^{\mathrm{TE,PC}}(\phi x)\frac{1 - 1/(AJ)}{1 - 1/(AH)}$$

where

$$A = \frac{\tilde{j}_l'(\sqrt{\varepsilon}\phi x)}{j_l(\sqrt{\varepsilon}\phi x)}; \quad J = \frac{j_l(\phi x)}{\tilde{j}_l'(\phi x)}; \quad H = \frac{h_l^{(1)}(\phi x)}{\tilde{h}_l^{(1)\prime}(\phi x)}.$$

With the assumption $\mathrm{Im}\{\sqrt{\varepsilon}\}\phi x \gg 1$, the asymptote (A1) leads to

$$\frac{\tilde{\jmath}_l'(\sqrt{\varepsilon}\phi x)}{\tilde{\jmath}_l(\sqrt{\varepsilon}\phi x)} \approx \sqrt{\varepsilon}\phi x \cot(\sqrt{\varepsilon}\phi x - \tfrac{l\pi}{2}) \approx -i\sqrt{\varepsilon}\phi x.$$

Using the asymptotes (A3) and (A4), we further have

$$\frac{j_l(\phi x)}{\tilde{\jmath}_l'(\phi x)} \approx \frac{1}{l+1}; \quad \frac{h_l^{(1)}(\phi x)}{\tilde{h}_l^{(1)\prime}(\phi x)} \approx -\frac{1}{l}$$

for $x \ll 1$. Combining these results and retaining only the next-to-leading order in x, one easily obtains Eqs. (3.23).

[1] J. Fortágh and C. Zimmermann, Rev. Mod. Phys. **79**, 235 (2007).
[2] S. Y. T. van de Meerakker, H. L. Bethlem, and G. Meijer, Nature Physics **4**, 595 (2008).
[3] T. F. Gallagher, *Rydberg Atoms* (Cambridge University Press, 1994).
[4] F. London, Zeitschr. Phys. **63**, 245 (1930).
[5] H. B. G. Casimir and D. Polder, Phys. Rev. **73**, 360 (1948).
[6] S. Y. Buhmann and D.-G. Welsch, Prog. Quantum Electron. **31**, 51 (2007).
[7] S. Scheel and S. Y. Buhmann, Acta Phys. Slov. **58**, 675 (2008).
[8] T. Nakajima, P. Lambropoulos and H. Walther, Phys. Rev. A **56**, 5100 (1997).
[9] S.-T. Wu and C. Eberlein, Proc. R. Soc. Lond. Ser. A **456**, 1931 (2000).
[10] M.-P. Gorza and M. Ducloy, Eur. Phys. J. D **40**, 343 (2006).
[11] M. Antezza, L. P. Pitaevskii, S. Stringari, and V. B. Svetovoy, Phys. Rev. A **77**, 022901 (2008).
[12] S. Y. Buhmann and S. Scheel, Phys. Rev. Lett. **100**, 253201 (2008).
[13] Y. Sherkunov, Phys. Rev. A **79**, 032101 (2009).
[14] G. Barton, Proc.R.Soc. London A **320**, 251 (1970); **367**, 117 (1979); **410**, 141 (1987).
[15] J. M. Wylie and J. E. Sipe, Phys. Rev. A **32**, 2030 (1985).
[16] W. Jhe, Phys.Rev. A **43**, 5795 (1991); **44**, 5932 (1991).
[17] S. Å. Ellingsen, Y. Sherkunov, S.Y. Buhmann, and S. Scheel, in *Proceedings of the Ninth Conference on Quantum Field Theory Under the Influence of External Conditions (QFEXT09)* edited by M. Bordag and K. A. Milton (World Scientific, 2010), p. 168, Preprint: `quant-ph/0910.5608`.
[18] S. Å. Ellingsen, S. Y. Buhmann, and S. Scheel, Phys. Rev. A **79**, 052903 (2009).
[19] J. A. Crosse, S. Å. Ellingsen, K. Clements, S. Y. Buhmann, and S. Scheel, Phys. Rev. A **82**, 010901(R) (2010); Erratum *ibid.* **82**, 029902(E) (2010).
[20] S. Å. Ellingsen, S. Y. Buhmann, and S. Scheel, Phys. Rev. Lett. **104**, 223003 (2010).
[21] S. Å. Ellingsen, S.Y. Buhmann, and S. Scheel, Preprint: `quant-ph/1106.5015` (2011).
[22] A. Weber and H. Gies, Phys. Rev. Lett. **105**, 040403 (2010).
[23] T. L. Ferrell and R. H. Ritchie, Phys. Rev. A **21**, 1305 (1980).
[24] A. M. Marvin and F. Toigo, Phys. Rev. A **25**, 782 (1982); **25**, 803 (1982).
[25] C. Girard, S. Maghezzi, and F. Hache, J. Chem. Phys. **91**, 5509 (1989).
[26] W. Jhe and J. W. Kim, Phys. Rev. A **51**, 1150 (1995).
[27] V. V. Klimov, M. Ducloy, and V.S. Letokhov, J. Mod. Opt. **43**, 2251 (1996).
[28] S. Y. Buhmann, H. T. Dung, and D.-G. Welsch, J. Opt. B: Quantum Semiclass. Opt. **6**, S127 (2004); Erratum: J. Phys. B: At. Mol. Opt. Phys. **39**, 3145 (2006).
[29] M. M. Taddei, T. N. C. Mendes and C. Farina, Eur. J. Phys. **31**, 89 (2010).
[30] A. Sambale, S. Y. Buhmann, and S. Scheel, Phys. Rev. A **81**, 012509 (2010).
[31] M. Babiker and G. Barton, J. Phys. A: Math. Gen. **9**, 129 (1976).
[32] I. Brevik, S. A. Ellingsen and K. A. Milton, New J. Phys. **8**, 236 (2006).
[33] S. Y. Buhmann, S. Scheel and J. Babington, Phys. Rev. Lett. **104**, 070404 (2010).
[34] M. Abramowitz and I. A. Stegun, *Handbook of Mathematical Functions* (Dover, New York, 1964).